Contents lists available at ScienceDirect

Asian Pacific Journal of Tropical Medicine

journal homepage: http://ees.elsevier.com/apjtm

Original research   http://dx.doi.org/10.1016/j.apjtm.2016.03.028
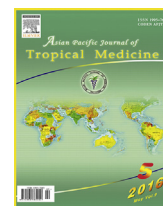
Zika Virus spreading in South America: Evolutionary analysis of emerging neutralizing resistant Phe279Ser strains

Marta Giovanetti[1,2,3], Teresa Milano[4], Luiz Carlos Alcantara[3], Laura Carcangiu[1], Eleonora Cella[1,5], Alessia Lai[6], Alessandra Lo Presti[1], Stefano Pascarella[4], Gianguglielmo Zehender[6], Silvia Angeletti[7], Massimo Ciccozzi[1,8*]

[1]*Department of Infectious Parasitic and Immunomediated Diseases, National Institute of Health, Rome, Italy*

[2]*Department of Biology, University of Rome 'Tor Vergata', Rome, Italy*

[3]*Laboratory of Hematology, Genetic and Computational Biology, Gonçalo Moniz Research Center, Oswaldo Cruz Foundation (LHGB/CPqGM/FIOCRUZ), Salvador, Bahia, Brazil*

[4]*Dipartimento di Scienze Biochimiche 'A. Rossi Fanelli', Università La Sapienza, 00185 Roma, Italy*

[5]*Department of Public Health and Infectious Diseases, Sapienza University of Rome, Rome, Italy*

[6]*Laboratory of Infectious Diseases and Tropical Medicine, University of Milan, Italy*

[7]*Clinical Pathology and Microbiology Laboratory, University Hospital Campus Bio-Medico of Rome, Rome, Italy*

[8]*University Campus Bio-Medico, Rome, Italy*

ARTICLE INFO

ABSTRACT

Objective: To investigate the genetic diversity of Zika Virus (ZIKV) and the relationships existing among these circulating viruses worldwide. To evaluate the genetic polymorphisms harbored from ZIKV that can have an influence on the virus circulation.
Methods: Three different ZIKV dataset were built. The first dataset included 63 *E* gene sequences, the second one 22 *NS3* sequences and the third dataset was composed of 108 *NS5* gene sequences. Phylogenetic and selective pressure analysis was performed. The edited nucleic acid alignment from the Envelope dataset was used to generate a conceptual translation to the corresponding peptide sequences through UGene software.
Results: The phylogeographic reconstruction was able to discriminate unambiguously that the Brazilian strains are belonged to the Asian lineage. The structural analysis reveals instead the presence of the Ser residue in the Brazilian sequences (however already observed in other previously reported ZIKV infections) that could suggest the presence of a neutralization-resistant population of viruses.
Conclusions: Phylogenetic, evolutionary and selective pressure analysis contributed to improve the knowledge on the circulation of ZIKV.

1. Introduction

Zika Virus (ZIKV) is an emerging mosquito-borne *Flavivirus* related to dengue, yellow fever, Japanese encephalitis, and West Nile viruses [1]. The genome of ZIKV is a single-stranded RNA of positive polarity of approximately 11 kb. Both ends of the genome contain the 5′ and the 3′ untranslated region, which do not encode for viral proteins. The encoded polyprotein is translated and co- and post-translationally processed by viral and cellular proteases into three structural proteins: capsid (C), pre-membrane (prM) or membrane (M), and envelope (E); seven non-structural proteins: NS1, NS2a, NS2b, NS3, NS4a, NS4b, and NS5. The NS5 protein is constituted by two distinct domains, an N-terminal methyltransferase and a C-terminal RNA-dependent RNA polymerase that are required for capping and synthesis of the viral RNA genome, respectively [2,3].

The virus is primarily transmitted through the bite of infected mosquitoes. It has been isolated from *Aedes africanus*, *Aedes apicoargenteus*, *Aedes luteocephalus*, *Aedes aegypti* (*Ae.*

aegypti), *Aedes vitatus*, and *Aedes furcifer* mosquitoes. *Aedes hensilii* was the predominant mosquito species found during the Yap islands outbreak in 2007 [4,5].

ZIKV has been documented in 1947, when it was isolated, for the first time, from a sentinel rhesus monkey stationed on a tree platform in the Zika forest, Uganda [6]. Since then, epizootics and small epidemics have occurred in Africa and Asia [4] until 2007 when a Zika fever epidemics took place in Yap Island, Micronesia [7].

ZIKV infection requires a differential diagnosis with other infectious such as Dengue and Chikungunya. After a short incubation period of few days, the symptoms appear and usually last from three to 12 d.

The symptoms are arbovirus-like can rash, fever, arthralgia, conjunctivitis, headache, vomiting and edema. The disease is acute but self-limiting. Frequently, the infection course can be asymptomatic [8,9]. The treatment is symptomatic, combining acetaminophen and antihistaminic drugs. Prevention against the infection, since there is no vaccine, relies on individual protection against bites and eradication of mosquitoes (anti-vectorial prevention).

Because of the lack of effective vaccines and/or therapies, ZIKV infection, can be considered an emerging disease and consequently a public health issue. In 2013, a large epidemic in French Polynesia was reported concomitantly with a dengue epidemic caused by serotypes 1 and 3. In the early 2015, records of patients presenting a 'dengue-like syndrome' appeared in Brazil. A new challenge has arisen in Brazil with the emergence of ZIKV and co-circulation with others arboviruses (*i.e.*, Dengue and Chikungunya virus). Improved surveillance and response measures are needed to mitigate the already burden on health systems in Brazil and limit further spread to other parts of the world.

In the present study, phylogenetic and evolutionary analyses have been performed to investigate the genetic diversity of ZIKV and the relationships existing among these circulating viruses worldwide. As a second aim, we evaluated the genetic polymorphisms harbored from ZIKV that can have an influence on the virus circulation.

2. Material and methods

2.1. Datasets

Three different ZIKV dataset were built. The first dataset included 63 *E* gene sequences, the second one 22 *NS3* sequences and the third dataset was composed of 108 *NS5* gene sequences. The sequences of all the dataset were downloaded from the National Center for Biotechnology Information (http://www.ncbi.nlm.nih.gov/). All of these dataset were used to perform the selective pressure analysis.

A subset of 57 *E* gene sequences with known sampling dates and location was built. The sampling dates for the sequences in this subset ranged from 1947 to 2015. The sampling locations were Brazil (BR = 6), Cambodia (KH, *n* = 1), Canada (CA = 1), Central African Republic (CF = 4), Cook Island (CK = 1), Côte D'ivoire (*CI* = 11), French Polynesia (PF = 1), Gabon (GA = 1), Malaysia (MY = 1), Micronesia (FM = 1), Nigeria (NG = 1), Senegal (SN = 26) and Uganda (UG = 2).

This subset was used, for the presence of the Brazilian strains, to trace the demographic history and the phylogeography

reconstruction related to the current epidemic in this South American country never reported before.

2.2. Likelihood mapping

The phylogenetic signal in a data set of aligned DNA or amino acid sequences can be investigated with the likelihood mapping method by analyzing groups of four sequences, randomly chosen, called quartets [10]. For a quartet, just three unrooted tree topologies are possible. The likelihood of each topology is estimated with the maximum likelihood method and the three likelihoods are reported as a dot in an equilateral triangle (the likelihood map).

Three main areas in the map can be distinguished: the three corners representing fully resolved tree topologies, *i.e.* the presence of treelike phylogenetic signal in the data; the center, which represents star-like phylogeny, and the three areas on the sides indicating network-like phylogeny, *i.e.* presence of recombination or conflicting phylogenetic signals. Extensive simulation studies have shown that >33% dots falling within the central area indicate substantial star-like signal, *i.e.* a star-like outburst of multiple phylogenetic lineages [10,11]. Likelihood mapping analyses were performed, on each dataset, with the program TREE-PUZZLE by analyzing 10 000 random quartets.

2.3. Bayesian phylogenetic analysis: demographic history and phylogeographic reconstruction

The sequences of all the dataset were aligned by using Clustal X and manually edited by Bioedit, as already described [12]. The evolutionary model was chosen as the best-fitting nucleotide substitution model in accordance with the results of the hierarchical likelihood ratio test implemented in Modeltest software version 3.7 as already described [13].

Maximum Clade Credibility tree on the subset (57 envelope gene sequences with known sampling date and location), were inferred using a Markov Chain Monte Carlo (MCMC) Bayesian approach implemented on the program BEAST v1.8, under HKY + Γ + I model estimating the evolutionary rate using both a strict and an uncorrelated log-normal relaxed clock model. As coalescent priors, three parametric demographic models of population growth (constant size, exponential, expansion) and a Bayesian skyline plot (a non-parametric piecewise-constant model) were compared. The best fitting models were selected by means of a Bayes factor (BF, using marginal likelihoods) implemented in Beast v 1.8 [14]. In accordance with Kass and Raftery [15] the strength of the evidence against H_0 (null hypothesis) was evaluated as follows: 2lnBF <2 = no evidence; 2–6 = weak evidence; 6–10 = strong evidence; and >10 = very strong evidence. A negative 2lnBF indicates evidence in favor of H_0. Only values of ≥ 6 were considered significant. The MCMC chains were run for at least 50 million generations, and sampled every 5 000 steps. Convergence was assessed on the basis of the effective sampling size. Only effective sampling size values of >250 were accepted. Uncertainty in the estimates was indicated by 95% highest posterior density (95% HPD) intervals. Statistical support for specific clades was obtained by calculating the posterior probability of each monophyletic clade.

The continuous time Markov Chain process over discrete sampling locations implemented in BEAST 1.8 [16] was used

for the phylogeographical analysis by implementing the Bayesian Stochastic Search Variable Selection model, which allows diffusion rates to be zero with a positive prior probability. The maximum clade credibility tree (the tree with the largest product of posterior clade probabilities) was selected from the posterior tree distribution after a 10% burn-in using the Tree Annotator program version 1.8. The final trees were manipulated in FigTree version 1.4.2 for display purposes.

The demographic history was analyzed on the subset by performing the Bayesian skyline plot.

2.4. Selective pressure analysis

The CODEML program implemented in the PAML 3.14 software package (http://abacus.gene.ucl.ac.uk/software/paml.html) was used to investigate the adaptive evolution of the Zika Virus genes (*E*, *NS3* and *NS5*). The sequences alignments of the three dataset were used to test whether they were under positive selection.

Six models of codon substitution: M0 (one-ratio), M1a (nearly neutral), M2a (positive selection), M3 (discrete), M7 (beta), and M8 (beta and omega) were used in this analysis [17]. Since these models are nested, we used codon-substitution models to fit the model to the data using the likelihood ratio test [18]. The discrete model (M3), with three dN/dS (ω) classes, allows ω to vary among sites by defining a set number of discrete site categories, each with its own ω value. Through maximum-likelihood optimization, it is possible to estimate the ω and *P* values and the fraction of sites in the aligned data set that falls into a given category. Finally, the algorithm calculates the a posteriori probability of each codon belonging to a particular site category. Using the M3 model, sites with a posterior probability exceeding 90% and a ω value >1.0 were designated as being 'positive selection sites' [17]. The site rate variation was evaluated comparing M0 with M3, while positive selection was evaluated comparing M1 with M2. The Bayes empirical Bayes approach implemented in M2a and M8 was used instead to determine the positively selected sites by calculating the posterior probabilities (*P*) of ω classes for each site [19]. It is worth noting that PAML likelihood ratio tests have been reported to be conservative for short sequences (*e.g.* positive selection could be underestimated), although the Bayesian prediction of sites under positive selection is largely unaffected by sequence length [18,20]. The dN/dS rate (ω) was also estimated by the ML approach implemented in the program HyPhy [21]. In particular, the global (assuming a single selective pressure for all branches) and the local (allowing the selective pressure to change along every branch) models were compared by likelihood ratio test. Site-specific positive and negative selection were estimated by two different algorithms: the fixed-effects likelihood, which fits an ω rate to every site and uses the likelihood ratio to test if dN = dS; and random effect likelihood, a variant of the Nielsen–Yang approach [22], which assumes that a discrete distribution of rates exists across sites and allows both dS and dN to vary independently site by-site. The two methods have been described in more detail elsewhere [23]. In order to select sites under selective pressure and keep our test conservative, a *P* value of ≤0.1 or a posterior probability of ≥0.9 as relaxed critical values [23] was assumed.

2.5. Protein sequence and structure analysis

The edited nucleic acid alignment from the Envelope dataset was used to generate a conceptual translation to the corresponding peptide sequences through UGene software [24]. The reference sequence of the ZIKV Envelope protein (Reference Sequence accession: NC_012532.1) for its entire lengths was then aligned, using Clustal X, to the translated protein alignment. Candidate templates for homology modeling, with the reference sequence ZIKV Envelope as a query, were assessed through the Phyre v2.0 server for protein fold recognition [25] and selected on the basis of query coverage, E-value and better quality of the template structures. The model of ZIKV Envelope protein was built based on the known structures of the homologous Envelope proteins from the Japanese Encephalitis virus (PDB ID: 3P54) and from the Dengue virus type 3 (Dt3) (PDB ID: 1UZG). Clustal X calculated the alignment of the target sequence with the selected templates. A total of ten homology models was generated and optimized using Modeller 9.13 [26]. The model with the best values of the Modeller scoring function was chosen for subsequent analysis. To remove unfavorable contacts of amino acid side chains, derived from the homology modeling process, energy minimization was applied to the selected model using the GROMOS96 force-field implementation in Swiss-PDB Viewer software (version 4.0.1) [27]. The model was validated with standard programs such as Prosa II and Procheck [28]. Residue conservation was evaluated through the Consurf server [29]. Alignment display and editing relied on UGene or Jalview [30] programs. Sequence Logos were drawn using WebLogo [31]. Protein structure analysis, in silico mutagenesis and mapping of the single point amino acid substitutions of the Brazilian Envelope protein sequences onto the three dimensional model and figure design were performed using PyMOL [32].

3. Results

3.1. Likelihood mapping

The phylogenetic noise of the three different dataset was investigated by means of likelihood mapping. The percentage of dots falling in the central area of the triangles was 6.9% for the first dataset (*Envelope* gene), 1.7% for the second dataset (*NS3* gene) and 15.8% for the third dataset (*NS5* gene); as none of the dataset showed more than 33% of noise, all of them contained sufficient phylogenetic signal.

3.2. Bayesian phylogenetic analysis: demographic history and phylogeographic reconstruction

The BF analysis for the subset showed that the relaxed clock fitted the data significantly better than the strict clock (2lnBF = 15.02 for relaxed clock). Under the relaxed clock the BF analysis showed that the skyline model was better than the other models (2lnBF > 24.568). The estimated mean value of the Zika Virus *E* gene evolutionary rate was of 4.04×10^{-4} substitution/site/year (95% HPD: 1.32×10^{-4}–7.41×10^{-4}).

Figure 1 showed the Bayesian phylogeographic tree of the *E* gene (subset) that was constructed using the evolutionary rate

estimated. Phylogeographic reconstruction showed that the highest state probability for the root of the tree was an African state, as already described (state probability, SP = 0.28). Phylogeographic reconstruction showed three statistically supported clade (Clade A, B, C), originated in Senegal (Clade A, SP = 0.51) in Malaysia (Clade B, SP = 0.30), in Côte D'ivoire (Clade C, SP = 0.46), which inside of them some clusters statistically supported appear.

Phylogeographic reconstruction was able to determine that the ZIKV virus outbreak has a single origin and is associated with the Asian phylogenetic clade. Our results are in line with a recent paper, which suggests that the single origin of the ZIKV outbreak in Brazil is from French Polynesia [33].

The demographic history of the first dataset of Zika Virus suggest that the epidemic showed a slight exponential growth up to 2 000 of the epidemic when started a decreasing phase showing a typical 'bottle neck' (Figure 2).

3.3. Evolutionary analysis

Selection pressure analyses performed in all the three different datasets *E*, *NS3* and *NS5* genes uncovered several sites
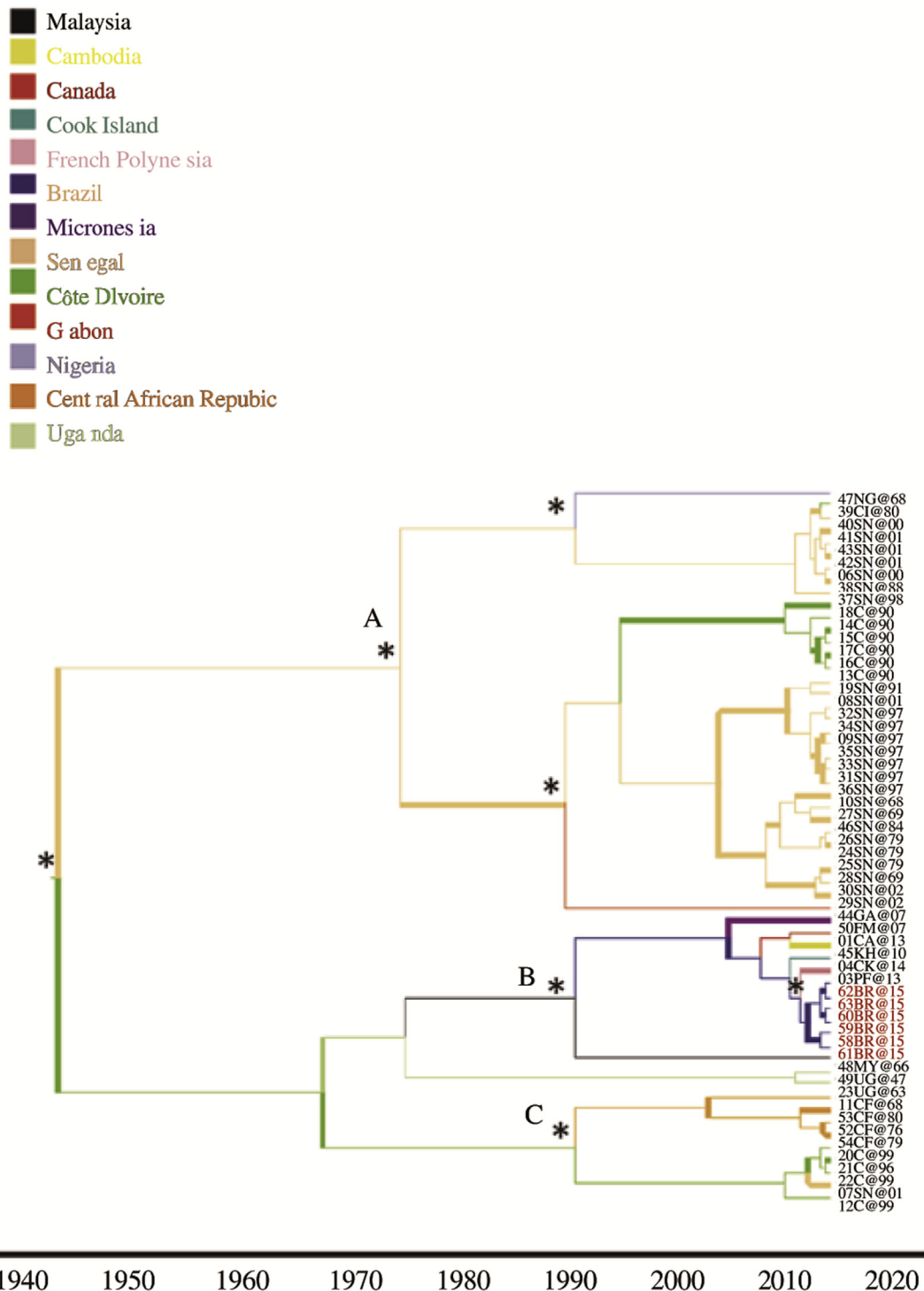

Figure 1. Bayesian phylogeographic tree of Zika Virus *E* gene sequences.
The branches are colored on the basis of the most probable state location of the descendent nodes. *: significant statistical support for the clade subtending that branch (*P* > 0.98). Locations are indicated in different colors. Brazilian strains are in red.
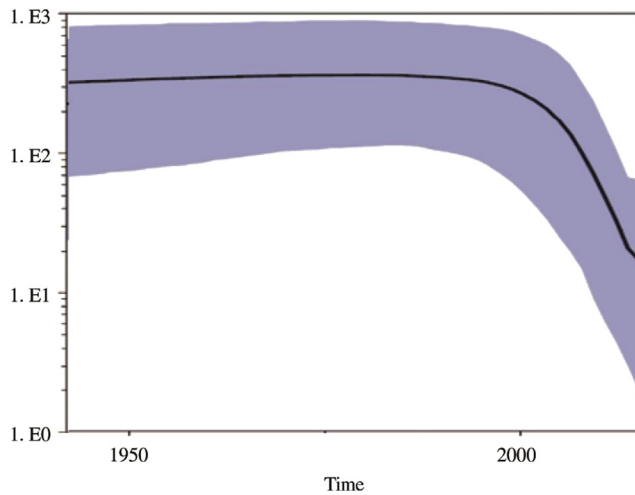
Figure 2. Bayesian skyline plot of the first dataset *E* gene of Zika Virus. The effective number of infections is reported on the Y-axis. Time is reported in the X-axis. The colored area corresponds to the credibility interval based on 95% highest HPD.

(59.57%, 49.81% and 39.55% for *E*, *NS3* and *NS5* datasets, respectively) under strong negative selection (by using HYPHY) indicated by $\omega < 0$ suggesting high degree conservation in the genomic region analyzed.

Likewise, the lack of positively selected sites, (both by using HYPHY and PAML), indicated by $\omega > 0$, is typical of highly adapted phenotypes and shows no detectable directional change on the available data. Likelihood values and parameter estimates obtained from different data sets are listed in Table 1. Estimates of the transition/transversion rate ratio (ts/tv) are quite homogeneous among models in each data set and thus are not shown in Table 1. The average ω ratio ranged from 0.0555 to 0.0674 among all models, for *E* gene dataset, suggesting that a non-synonymous mutation has only 5.55%–6.74% as much chance as a synonymous mutation of being fixed in the population. Regarding NS3 dataset the ω ratio ranged from 0.0538 to 0.0754 suggesting that a non-

synonymous mutation has only 5.58%–7.54% as much chance as a synonymous mutation of being fixed in the population. Finally the average ω ratio for NS5 dataset ranged from 0.062 to 0.102 suggesting that a non-synonymous mutation has only 6.2%–1.02% as much chance as a synonymous mutation of being fixed in the population.

3.4. Protein sequence and structure analysis

The alignment of Envelope proteins pointed out two sites where a residue substitution in the Brazilian sequences with respect to the others can be observed. The Phe in position 279 (numbering refers to the complete ZIKV reference sequence) is replaced by a Ser, while in position 311 an Ile is observed in place of a Val. As in the Brazilian sequence, both substitutions are present in other Envelope protein sequences: more precisely, in the sequences from virus strains isolated in Canada, Cambodia, Malaysia, French Polynesia, Micronesia and Cook Islands (Figure 3A). Except the Malaysian sequence, all the others date back to the last decade.

Residue conservation analysis carried out through Consurf site, revealed that residues occupying position 279 and 311 of ZIKV reference sequence are not conserved throughout protein sequences of Envelope proteins, independently from their origin (however, it should be noted that only sequences from flavivirus were selected). These amino acidic positions were mapped onto the three-dimensional structure of the Envelope protein homology model superposed to the original template from Dengue type 3 (Figure 3B). The side chains of both residues are located on the surface of the E protein, and probably for this reason they are predicted to be not essential for the maintenance of appropriate protein fold (*i.e.* the mutations do not destabilize the structure).

Ser 279 is located at the boundary between the so-called Domain I (DI), the central domain, and the Domain II (DII) (Figure 3B). In the template structures, a Phe residue, as well as in most of ZIKV Envelope proteins, occupies the same position.

Table 1

Likelihood values and parameters estimates for the selection analysis of the *E* and *NS3* and *NS3* gene.

|	Model code	lnL	dN/dS	Estimates of parameters
E	M_0 one ratio	−1 171.27	0.0555	$\omega = 0.0555$
	M_1 neutral	−1 166.52	0.0674	$P_0 = 0.97187$, $(P_1 = 0.02813)$
	M_2 selection	−1 166.46	0.0674	$P_0 = 0.97186$, $P_1 = 0.02814$ $(P_2 = 0.00000)$, $\omega_2 = 16.30422$
	M_3 discrete	−1 166.34	0.0641	$P_0 = 0.95474$, $P_1 = 0.04526$ $(P_2 = 0.00000)$
				$\omega_0 = 0.03579$, $\omega_1 = 0.66085$, $\omega_2 = 37.92208$
	M_7 beta	−1 167.38	0.0620	$P = 0.28159$, $q = 3.99166$
	M_8 beta and ω	−1 167.45	0.0620	$P_0 = 1.00000$ $(P_1 = 0.00000)$, $P = 0.28160$, $q = 3.99197$, $\omega = 6.57800$
NS3	M_0 one ratio	−2 916.60	0.0538	$\omega = 0.0538$
	M_1 neutral	−2 900.21	0.0754	$P_0 = 0.95519$, $(P_1 = 0.04481)$
	M_2 selection	−2 900.21	0.0754	$P_0 = 0.95519$, $P_1 = 0.02239$ $(P_2 = 0.02242)$, $\omega_2 = 1.00000$
	M_3 discrete	−2 892.53	0.0585	$P_0 = 0.70707$, $P_1 = 0.24390$, $(P_2 = 0.04903)$
				$\omega_0 = 0.00000$, $\omega_1 = 0.13814$, $\omega_2 = 0.50559$
	M_7 beta	−2 892.78	0.0581	$P = 0.13890$ $q = 2.04982$
	M_8 beta and ω	−2 892.78	0.0581	$P_0 = 1.00000$, $(P_1 = 0.00000)$, $P = 0.13890$, $q = 2.04986$, $\omega = 1.00000$
NS5	M_0 one ratio	−3 973.48	0.062	$\omega = 0.062$
	M_1 neutral	−3 955.75	0.102	$P_0 = 0.92882$, $(P_1 = 0.07118)$
	M_2 selection	−3 955.75	0.102	$P_0 = 0.92882$, $P_1 = 0.07118$ $(P_2 = 0.00000)$ $\omega_2 = 9.45147$
	M_3 discrete	−3 903.66	0.080	$P_0 = 0.30774$, $P_1 = 0.61422$ $(P_2 = 0.07804)$
				$\omega_0 = 0.00000$, $\omega_1 = 0.06181$, $\omega_2 = 0.53959$
	M_7 beta	−3 912.88	0.080	$P = 0.35145$, $q = 3.85074$
	M_8 beta and ω	−3 912.88	0.080	$P_0 = 1.00000$, $(P_1 = 0.00000)$, $P = 0.35140$ $q = 3.84973$, $\omega = 6.27537$
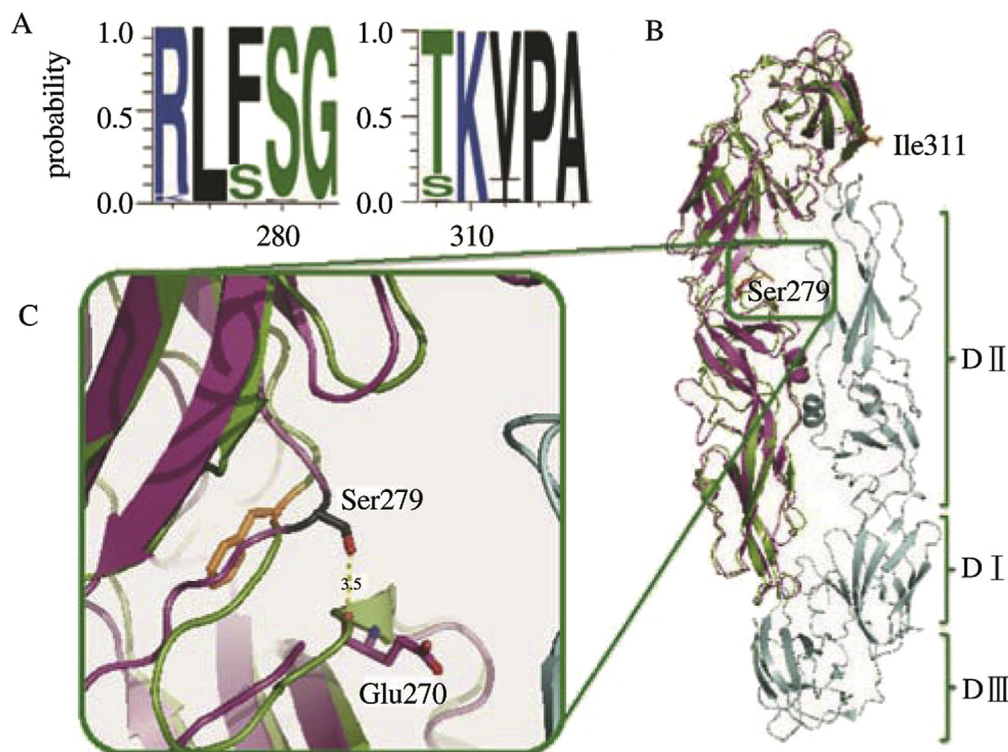
Figure 3. Mapping of residue characteristic of Brazilian sequences on the Envelope protein of ZIKV A.
Logos of ZIKV E proteins. Logos were obtained from the alignment of ZIKV E protein sequences. Residues are represented with the one-letter code. X-axis indicates sequence position. The overall height of each letter stack indicates the sequence conservation at that position, while the height of symbols within the stack indicates the relative frequency of each amino or nucleic acid at that position. Colors reflect chemical-physical residue properties. Here, only the ZIKV E regions encompassing the Phe279Ser and Ile311 are shown.

Comparison of the amino acid sequences of other flavivirus E proteins, carried out with Consurf analysis, indicated that Phe279 was conserved in most wild-type viruses, although surrounding residues varied. The transition from a hydrophobic to a polar residue, as it is the case of Brazilian sequences, alter the local charge of the pocket: indeed, manual inspection of the structure showed a polar contact (Figure 3C), not observed in the wild type structure, between Ser side chain and the peptide carbonyl oxygen of a conserved Glu residue.

Regarding the other position that appears to be characteristic of Brazilian E sequences, Ile311Val, it should be observed that the position is highly variable in the sequence alignment obtained with other flavivirus sequences. Indeed, looking at the template structure, the structurally equivalent position in Japanese Encephalitis virus and D3t Envelope are occupied by an Asn and a Glu residue, respectively. Moreover, inspection of the model revealed that the Val side chain is projected on the surface of the protein (Figure 3B) in a loop located in the Domain III, near to the interface with the other monomer of E protein. So far, no functional role was confirmed for this residue from previous studies.

4. Discussion

The application of high-resolution phylogenetic methods, such as the Bayesian statistical inference framework, can allow the reconstruction of the geographic history of the still ongoing and never reported before epidemic in Brazil on the basis of the first isolates sampled at known times. Phylogeographic analysis may contribute to better understand the epidemiological history,

the diffusion routes of this new epidemic and may contribute to the planning of prevention strategies [34].

Only few data are actually available regarding the phylogenies of Zika Virus in Brazil. Moreover there are limited sequences available in NCBI especially with regard to the still ongoing epidemic wave in this South American Country. In the present study the phylogenetic analysis was conducted including all sequences with location, available in GenBank. This is the first study that focusing on Brazilian strains, by the evolutionary and phylogeographic analysis of ZIKV, for the *E* gene.

The phylogeographic analysis showed that, Zika Virus was probably originated in Africa and spread following different routes to the other locations, including African (Senegal, Côte D'ivoire and Uganda) and Asian (Malaysia, Micronesia, French Polynesia) regions. The analysis confirmed the proposed designation of the two probable lineage Asian and African, that was first reported in 2012 [35].

For the first time, in this paper, the phylogeographic reconstruction was able to determine that the current ZIKV virus outbreak in Brazil has a single origin and is associated with the Asian phylogenetic clade. Our results seem also to be in line with a recent paper, which suggests that the single origin of the ZIKV outbreak in Brazil is from French Polynesia [33].

The phylodynamic analyses showed a slight exponential growth up to 2000 of the epidemic when started a decreasing phase showing a typical 'bottle neck' that could be explained with measures taken to reclaim [36].

Insecticide treatments have probably driven a selection on the population causing severe bottlenecks and the appearance of insecticide resistance in *Ae. aegypti* [37,38].

The genetic polymorphisms of ZIKV may also influence the virus circulation. Virus infectivity and antigenic variability and in particular, antigenic variation may play an important role in the ability of these viruses to escape the host immune response. In our study, using a selective pressure analysis method, negatively selected sites, were mostly found, suggesting the stability of the viral E, NS3 and NS5 proteins.

The alignment of Envelope proteins pointed out two sites where a residue substitution in the Brazilian sequences with respect to the others can be observed.

Ser 279 is located at the boundary between the so called Domain I, the central domain, and the Domain II, that contribute to important dimerization contacts that coordinate the antiparallel E arrangement on mature virus particle [39]. This region, defined as the 'kl' beta-hairpin binding pocket, has a role in the conformational rearrangement that drives membrane fusion [40]. In the template structures, a Phe residue, as well as in most of ZIKV Envelope proteins, occupies the same position. Comparison of the amino acid sequences of other flavivirus E proteins, carried out with Consurf analysis, indicated that Phe279 was conserved in most wild-type viruses, although surrounding residues varied. This conservation is in line with the function of the hydrophobic pocket, which through a conformational shift, is able to accept hydrophobic ligands [41]. The transition from a hydrophobic to a polar residue, as it is the case of Brazilian sequences, alter the local charge of the pocket: indeed, manual inspection of the structure showed a polar contact, not observed in the wild type structure, between Ser side chain and the peptide carbonyl oxygen of a conserved Glu residue. A similar Phe to Ser substitution in the equivalent position of the E protein of Dengue 3 virus was reported by Lee *et al.* [42]: they observed that this mutation causes escape from neutralization with IgM M10 and was associated with altered pH sensitivity of that virus. Moreover, the substitution of Ser for Phe at E279 of the dengue 1 neutralization-resistant virus population was demonstrated to be a nonconservative change that increased the hydrophilicity of this region of the protein [43]. A sort of analogy can be do with Chikungunya virus about the A226V of the E1 protein. Lo Presti *et al.* [44] followed this variant reconstructing the geographic spread of CHIKV during the last epidemic wave. This mutation was important and necessary to change the Chikungunya vector from *Ae. aegypti* to *Aedes albopictus* determining the Indian Ocean outbreak [44]. Because only few sequences have been available from Brazil it is important to follow and to confirm the eventual introduction of ZIKV in Brazil from Asian regions. A more extensive analysis of additional samples from other Brazilian regions, as well as a complete viral genetic characterization is needed.

All these observations suggest that, also in ZIKV Envelope, the region around Phe279Ser mutation might act as a hinge for low pH-induced conformational changes accompanying the E protein dimer to trimer transition, which occurs prior to its fusion with host cell membranes. The presence of the Ser residue in the Brazilian sequences (however already observed in other previously reported ZIKV infections) could suggest the presence of a neutralization-resistant population of viruses [45].

In conclusion, the study trough the phylogeographic and selective pressure analysis contributed to improve the knowledge on the circulation of ZIKV in Brazil. From these analysis emerged also the indication of a possible outbreak in Brazil with strains Phe279Ser neutralizing resistant that could indicate the need of a molecular epidemiological monitoring.

The understanding of the epidemiology of ZIKV is limited and the evolution of the outbreak needs to be carefully investigated to better assess the risk of spread and its consequences for public health. The knowledge of the circulating ZIKV lineages in Brazil is considered essential, as the Asian lineage seems to have a high epidemic potential.

Conflict of interest statement

We declare that we have no conflict of interest.

References

[1] World Health Organization (WHO). Zika virus outbreaks in the Americas. *Wkly Epidemiol Rec* 2015; **90**: 609-610.

[2] Chambers TJ, Chang HS, Galler R, Rice CM. Flavivirus genome organization, expression and replication. *Annu Rev Microbiol* 1990; **44**: 649-688.

[3] Kuno G, Chang GJJ. Full-length sequencing and genomic characterization of Bagaza, Kedougou, and Zika viruses. *Arch Virol* 2007; **152**: 687-696.

[4] Hayes EB. Zika virus outside Africa. *Emerg Infect Dis* 2009; **15**: 1347-1350.

[5] Marcondes CB, Ximenes MF. Zika virus in Brazil and the danger of infestation by *Aedes* (Stegomyia) mosquitoes. *Rev Soc Bras Med Trop* 2015 Dec 22; http://dx.doi.org/10.1590/0037-8682-0220-2015.

[6] Dick GW, Kitchen SF, Haddow AJ. Zika virus I. Isolations and serological specificity. *Trans R Soc Trop Med Hyg* 1952; **46**: 509-520.

[7] Duffy MR, Chen TH, Hancock WT, Powers AM, Kool JL, Lanciotti RS, et al. Zika virus outbreak on Yap Island, Federated States of Micronesia. *N Engl J Med* 2009; **360**: 2536-2543.

[8] Grard G. Zika virus in Gabon (Central Africa)-2007: a new threat from Aedes albopictus? *PLoS Negl Trop Dis* 2014; **8**: e2681.

[9] Gatherer D, Kohl A. Zika virus: a previously slow pandemic spreads rapidly through the Americas. *J Gen Virol* 2016; **97**(2): 269-273.

[10] Strimmer K, von Haeseler A. Likelihood-mapping: a simple method to visualize phylogenetic content of a sequence alignment. *Proc Natl Acad Sci USA* 1997; **94**: 6815-6819.

[11] Salemi M, de Oliveira T, Ciccozzi M, Rezza G, Goodenow MM. High-resolution molecular epidemiology and evolutionary history of HIV-1 subtypes in Albania. *PLoS One* 2008; **3**(1): e1390.

[12] Ciccozzi M, Vujošević D, Lo Presti A, Mugoša B, Vratnica Z, Lai A, et al. Genetic diversity of HIV type 1 in Montenegro. *AIDS Res Hum Retroviruses* 2011; **27**: 921-924.

[13] Ciccozzi M, Lai A, Ebranati E, Gabanelli E, Galli M, Mugosa B, et al. Phylogeographic reconstruction of HIV type 1B in Montenegro and the Balkan region. *AIDS Res Hum Retroviruses* 2012; **28**: 1280-1284.

[14] Drummond AJ, Rambaut A, Shapiro B, Pybus OG. Bayesian coalescent inference of past population dynamics from molecular sequences. *Mol Biol Evol* 2005; **22**: 1185-1192.

[15] Kass RE, Raftery AE. Bayes factors. *J Am Stat Assoc* 1995; **90**: 773-795.

[16] Lemey P, Rambaut A, Drummond AJ, Suchard MA. Bayesian phylogeography finds its roots. *PLoS Comput Biol* 2009; **5**: 1-16.

[17] Yang Z, Nielsen R, Goldman N, Pedersen AM. Codon substitution models for heterogeneous selection pressure at amino acid sites. *Genetics* 2000; **155**: 431-449.

[18] Anisimova M, Bielawsky JP, Yang Z. Accuracy and power of likelihood ratio test in detecting adaptive evolution. *Mol Biol Evol* 2001; **18**: 1585-1592.

[19] Yang Z, Wong WS, Nielsen R. Bayes empirical Bayes inference of amino acid sites under positive selection. *Mol Biol Evol* 2005; **22**: 1107-1118.

[20] Anisimova M, Bielawsky JP, Yang Z. Accuracy and power of Bayes prediction of amino acid sites under positive selection. *Mol Biol Evol* 2002; **19**: 950-958.

[21] Pond SL, Frost SD, Muse SV. HyPhy: hypothesis testing using phylogenies. *Bioinformatics* 2005; **21**: 676-679.

[22] Nielsen R, Yang Z. Likelihood models for detecting positively selected amino acid sites and applications to the HIV-1 envelope gene. *Genetics* 1998; **148**(3): 929-936.

[23] Kosakovsky Pond SL, Frost SD. Not so different after all: a comparison of methods for detecting amino acid sites under selection. *Mol Biol Evol* 2005; **22**: 1208-1222.

[24] Okonechnikov K, Golosova O, Fursov M. Unipro UGENE: a unified bioinformatics toolkit. *Bioinformatics* 2012; **28**(8): 1166-1167.

[25] Kelley LA, Mezulis S, Yates CM, Wass MN, Sternberg MJE. The Phyre2 web portal for protein modelling, prediction and analysis. *Nat Protoc* 2015; **10**: 845-858.

[26] Sali A, Blundell TL. Comparative protein modelling by satisfaction of spatial restraints. *J Mol Biol* 1993; **234**: 779-815.

[27] Kaplan W, Littlejohn TG. Swiss-PDB viewer (deep view). *Brief Bioinform* 2001; **2**: 195-197.

[28] Laskowski RA, Rullmannn JA, MacArthur MW, Kaptein R, Thornton JM. AQUA and PROCHECK-NMR: programs for checking the quality of protein structures solved by NMR. *J Biomol NMR* 1996; **8**: 477-486.

[29] Ashkenazy H, Erez E, Martz E, Pupko T, Ben-Tal N. ConSurf 2010: calculating evolutionary conservation in sequence and structure of proteins and nucleic acids. *Nucleic Acids Res* 2010; **38**(Suppl. 2): W529-W533.

[30] Waterhouse AM, Procter JB, Martin DMA, Clamp M, Barton GJ. Jalview version 2-a multiple sequence alignment editor and analysis workbench. *Bioinformatics* 2009; **25**: 1189-1191.

[31] Crooks GE, Hon G, Chandonia JM, Brenner SE. WebLogo: a sequence logo generator. *Genome Res* 2004; **14**: 1188-1190.

[32] Schroedinger L. *The PyMOL molecular graphics system, version 1.7.4.* Schrödinger, LLC; 2015.

[33] Musso D. Zika virus transmission from French Polynesia to Brazil. *Emerg Infect Dis* 2015; **21**: 1887.

[34] Pybus OG, Rambaut A. Evolutionary analysis of the dynamics of viral infectious disease. *Nat Rev Genet* 2009; **10**: 540-550.

[35] Haddow AD, Schuh AJ, Yasuda CY, Kasper MR, Heang V, Huy R, et al. Genetic characterization of Zika virus strains: geographic expansion of the Asian lineage. *PLoS Negl Trop Dis* 2012; **6**(2): e1477.

[36] Herrera F, Urdaneta L, Rivero J, Zoghbi N, Ruiz J, Carrasquel G, et al. Population genetic structure of the dengue mosquito *Aedes aegypti* in Venezuela. *Mem Inst Oswaldo Cruz* 2006; **101**: 625-633.

[37] Bisset JA, Rodriguez MM, Molina D, Diaz C, Soca LA. High esterases as mechanism of resistance to organophos-phate insecticides in *Aedes aegypti* strains. *Rev Cubana Med Trop* 2001; **53**: 37-43.

[38] Rodriguez MM, Bisset J, de Fernandez DM, Lauzan L, Soca A. Detection of insecticide resistance in *Aedes aegypti* (Diptera: Culicidae) from Cuba and Venezuela. *J Med Entomol* 2001; **38**: 623-628.

[39] Rey FA, Heinz FX, Mandl C, Kunz C, Harrison SC. The envelope glycoprotein from tick-borne encephalitis virus at 2 A resolution. *Nature* 1995; **375**: 291-298.

[40] Modis Y, Ogata S, Clements D, Harrison SC. Structure of the dengue virus envelope protein after membrane fusion. *Nature* 2004; **427**: 313-319.

[41] Modis Y, Harrison SC. A ligand-binding pocket in the dengue virus envelope glycoprotein. *Proc Natl Acad Sci USA* 2003; **100**: 6986-6991.

[42] Lee E, Weir RC, Dalgarno L. Changes in the dengue virus major envelope protein on passaging and their localization on the three-dimensional structure of the protein. *Virology* 1997; **232**: 281-290.

[43] Beasley DW, Aaskov JG. Epitopes on the dengue 1 virus envelope protein recognized by neutralizing IgM monoclonal antibodies. *Virology* 2001; **279**: 447-458.

[44] Lo Presti A, Ciccozzi M, Cella E, Lai A, Simonetti FR, Galli M, et al. Origin, evolution, and phylogeography of recent epidemic CHIKV strains. *Infect Genet Evol* 2012; **12**: 392-398.

[45] Pierson TC, Kielian M. Flaviviruses: braking the entering. *Curr Opin Virol* 2013; **3**: 3-12.